

The g^6 pressure of hot Yang-Mills theory: Canonical form of the integrand

Pablo Navarrete^{a,b} and York Schröder^a

^a*Centro de Ciencias Exactas, Departamento de Ciencias Básicas, Universidad del Bío-Bío, Avenida Andrés Bello 720, Chillán, Chile*

^b*Department of Physics and Helsinki Institute of Physics, P.O. Box 64, University of Helsinki, Finland*

E-mail: pablo.navarrete@helsinki.fi, yschroder@ubiobio.cl

ABSTRACT: We present major progress towards the determination of the last missing piece for the pressure of a Yang-Mills plasma at high temperatures at order g^6 in the strong coupling constant. This order is of key importance due to its role in resolving the long-standing infrared problem of finite-temperature field theory within a dimensionally reduced effective field theory setup. By systematically applying linear transformations of integration variables, or momentum shifts, we resolve equivalences between different representations of Feynman sum-integrals on the integrand level, transforming those into a canonical form. At the order g^6 , this results in reducing a sum of $\mathcal{O}(100000)$ distinct sum-integrals which are produced from all four-loop vacuum diagrams down to merely 21. Furthermore, we succeed to map 11 of those onto known lower-loop structures. This leaves only 10 genuine 4-loop sum-integrals to be evaluated, thereby bringing the finalization of three decades of theoretical efforts within reach.

KEYWORDS: Higher-Order Perturbative Calculations, Effective Field Theories of QCD, Renormalization and Regularization, Thermal Field Theory

ARXIV EPRINT: [2408.15830](https://arxiv.org/abs/2408.15830)

Contents

1	Introduction	1
2	Setup	2
3	Reduction to canonical form	4
3.1	Mapping	5
3.2	Canonical form	7
3.3	Bare pressure at g^6	8
4	Sum-integral evaluations	8
4.1	Factorized sectors: one loop	9
4.2	Factorized sectors: two loops	9
4.3	Factorizable sectors: three loops	9
4.4	Non-factorized sectors	10
5	Conclusions	12
A	Bare pressure up to g^4	13
B	Massless bosonic vacuum sum-integrals	14
B.1	One loop	14
B.2	Two loops	15
B.3	Three loops	15
B.4	Four loops	16

1 Introduction

It had been argued [1–3] and indeed widely accepted [4, 5], that a weak-coupling expansion of hot QCD can not be consistently performed. The argument rests on the observation that transverse (“chromomagnetic”) gluonic modes that remain unscreened when propagating through the hot plasma cause an infrared problem, which for the pressure arises at four loops and beyond.

Based on more recent understanding of effective field theory, however, a roadmap to evade this infrared problem in the setting of dimensionally reduced effective theories [6–8] has been laid out in a seminal paper [9]. This has spurred enormous theoretical efforts [10–19], completing most but one of the required steps. The one missing piece of information is a well-defined perturbative coefficient in hot QCD, at the four-loop level.

As the root cause of the infrared problem lies in the gluonic sector of QCD, we set the number of fermions $N_f = 0$ in this work and focus on the pure Yang-Mills case, as already

suggested by the manuscript’s title. The addition of fermions does not present any new fundamental problems, and might be classified as more of a bookkeeping exercise. Indeed, weak-coupling results for full QCD up to g^5 have been known for a long time [20–26], and been partially extended to the four-loop level at large N_f [27], with those $N_f \neq 0$ corrections generally exhibiting very good convergence properties, in contrast to the situation at $N_f = 0$ [9, 26, 28–30].

There are order-of-magnitude numerical estimates at $N_f = 0$ of the above-mentioned missing perturbative coefficient [18, 30, 31] based on comparisons with non-perturbative lattice Monte Carlo simulations of pure Yang-Mills theory [32–35] at a scale where both approaches might still be applicable. To appreciate why a diagrammatic evaluation of this coefficient is still missing to date, it is instructive to simply count the number of terms that appear in the (sum-) integrand of purely gluonic 4-loop vacuum Feynman diagrams, after multiplying out the vertex- (6 terms per gluon 3-vertex) and propagator- (2 terms per gluon propagator) structures. For example, diagrams that contain gluon-3-vertices only (see lines 6 and 7 of figure 3 for concrete examples) contain 6 vertices and 9 propagators, leading to $6^6 \times 2^9 \approx 24$ million terms each before combining equal terms.

The main focus of the present paper is to tackle this open perturbative problem head on, organizing the enormous number of terms that appear in the 4-loop expansion of the Yang-Mills pressure in general covariant gauges. To this end, we propose an algorithm that makes systematic use of momentum shift invariance, enabling us to define a canonical form on the integrand level. As a result, we manage to eliminate redundancy among equivalent (sum-) integral representations, observing an enormous reduction in expression size of the 4-loop problem, and even obtaining gauge parameter independence as a welcome by-product. Furthermore, we map some of the remaining canonicalized integrals onto known factorized cases, and close by precisely defining a few open calculations that would be needed to finish the roadmap that had been sketched almost three decades ago [9].

The structure of the remainder of the paper is as follows. We start by defining the observable in question and introduce some useful related notation in section 2. Details of our computation regarding the canonicalization and the mapping onto factorized sum-integrals are explained in sections 3 and 4, respectively. We conclude in section 5, and devote two appendices to collect information on lower-loop coefficients as well as relevant known cases of sum-integral evaluations.

2 Setup

The above-mentioned dimensionally reduced effective theory setup that enables a high-temperature weak-coupling expansion of the full QCD pressure¹

$$p_{\text{QCD}}(T) = \lim_{V \rightarrow \infty} \frac{T}{V} \ln \int \mathcal{D}[A, \bar{\psi}, \psi] \exp \left(- \int_0^{1/T} d\tau \int d^d \mathbf{x} L_{\text{QCD}}^{\text{E}} \right) \quad (2.1)$$

¹The pressure is an equilibrium quantity, so we work in the imaginary-time formalism [36] with Euclidean Lagrange density $L_{\text{QCD}}^{\text{E}}$ that results after rotating $t \rightarrow i\tau$. Bosons (fermions) are (anti)periodic in τ .

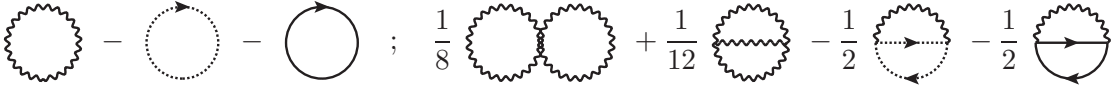


Figure 1. Left panel: Feynman diagrams contributing to the leading-order term of the QCD pressure, p_0 of eq. (2.2). Wiggly, dotted and full lines represent gluons, ghosts and quarks, respectively. Right panel: Two-loop Feynman diagrams contributing to p_2 of eq. (2.2).

in terms of distinct contributions from three formally well-separated (so-called hard, soft and ultrasoft) momentum scales has been described in many places [9, 30, 31]. It leads to the three-term separation $p_{\text{QCD}} = p_{\text{hard}} + p_{\text{soft}} + p_{\text{ultrasoft}}$, where the first two are perturbative and the last is not. We will not repeat the details of this systematic decomposition here, but focus directly on the key remaining open problem, being the determination of the 4-loop term in a strict² perturbative expansion of p_{QCD} in terms of the bare gauge coupling g_{B}^2 . This specific coefficient arises from the hard momentum scales and is sometimes referred to as β_{E1} in the literature [30].

For an $\text{SU}(N_c)$ gauge group, we write the relevant perturbative expansion as

$$p_{\text{hard}}^{\text{bare}} = p_0 + g_{\text{B}}^2 N_c p_2 + g_{\text{B}}^4 N_c^2 p_3 + g_{\text{B}}^6 N_c^3 p_4 + \mathcal{O}(5\text{-loop}) . \quad (2.2)$$

The free gauge theory gives rise to the ideal-gas term $p_0 = \frac{\pi^2 T^4}{45} [(N_c^2 - 1) + \frac{7}{4} N_c N_f]$ whose value can be obtained³ from the first three 1-loop diagrams shown in figure 1. Interactions then give rise to the 2-loop correction p_2 [20, 21], the 3-loop term p_3 [24, 25], and p_4 at four loops which contains β_{E1} . We show all Feynman diagrams that make up p_2 and p_3 in figures 1 and 2, while for p_4 we display only the pure-gauge part in figure 3. A concise review of the known coefficients up to three loops is presented in [37]. Below, we provide analytic expressions for the p_n , for d dimensions and at $N_f = 0$, where $p_4(N_f = 0)$ constitutes the main new result of our paper. For completeness, we note that in full QCD the 4-loop term receives four separate contributions that may be indexed by the respective power of N_f as $p_4 = p_{40} + N_f p_{41} + N_f^2 p_{42} + N_f^3 p_{43}$. Of these, only p_{43} can be considered known since it can be extracted at large N_f [38, 39] or from a single Feynman diagram [27]. To re-iterate, we focus on p_{40} here.

Let us fix some notation. Due to the compact temporal integration domain in eq. (2.1), Fourier transforming to momentum space leads to a tower of discrete (Matsubara) frequencies that need to be summed over. We employ Euclidean four-momenta $K = (K_0, \mathbf{k})$, where the components $K_0 = 2n_k \pi T$ are bosonic Matsubara frequencies with $n_k \in \mathbb{Z}$. Massless (bosonic) propagators are then $1/[K^2] = 1/[(K_0)^2 + \mathbf{k}^2]$, and we define the sum-integral symbol as

$$\oint_K \equiv T \sum_{n_k \in \mathbb{Z}} \int \frac{d^d \mathbf{k}}{(2\pi)^d} , \quad (2.3)$$

²That is, disregarding the known infrared divergences that persist even in the sum of all bare diagrams at that order, but regularizing them together with the ultraviolet ones within dimensional regularization.

³Famously, the ghost corrects the overcounting in the partition function due to the gluonic degrees of freedom as $p_0 = \frac{\pi^2 T^4}{45} (N_c^2 - 1) [2 - 1 + \mathcal{O}(N_f)]$, where the contributions shown in square brackets originate from the first three diagrams of figure 1, in order.

$$\begin{aligned}
& +\frac{1}{16} \text{diagram} + \frac{1}{48} \text{diagram} + \frac{1}{8} \text{diagram} - \frac{1}{4} \text{diagram} + \frac{1}{8} \text{diagram} + \frac{1}{24} \text{diagram} \\
& -\frac{1}{3} \text{diagram} - \frac{1}{4} \text{diagram} + \frac{1}{16} \text{diagram} - \frac{1}{4} \text{diagram} + \frac{1}{4} \text{diagram} - \frac{1}{2} \text{diagram} \\
& -\frac{1}{4} \text{diagram} - \frac{1}{4} \text{diagram} - \frac{1}{3} \text{diagram} - \frac{1}{4} \text{diagram} + \frac{1}{2} \text{diagram} - \frac{1}{2} \text{diagram} + \frac{1}{4} \text{diagram}
\end{aligned}$$

Figure 2. Three-loop Feynman diagrams contributing to p_3 of eq. (2.2). The first two lines depict purely bosonic diagrams making up $p_3(N_f = 0)$, while the third line shows the diagrams proportional to N_f and N_f^2 (last diagram only). Notation as in figure 1.

where $d = 3 - 2\varepsilon$ reflects dimensional regularization.

To facilitate the analysis of all momentum-space vacuum Feynman (sum-) integrals that contribute to p_4 , we use a fixed set of massless 4-loop propagators constructed from squares of the ten linear combinations P_a^μ of the four loop momenta $K_1^\mu \dots K_4^\mu$ given by (we omit Lorentz indices and write $K_{i-j} \equiv K_i - K_j$)

$$\{P_1, \dots, P_{10}\} = \{K_1, K_2, K_3, K_4, K_{1-4}, K_{2-4}, K_{3-4}, K_{1-2}, K_{1-3}, K_{1-2-3}\}. \quad (2.4)$$

This allows to express any scalar bosonic 4-loop vacuum sum-integral, as needed for the diagrams shown in figure 3, as a list of 10 numbers $s_a \in \mathbb{Z}$ as

$$\mathcal{I}(s_1, \dots, s_{10}) \equiv \oint_{K_1} \oint_{K_2} \oint_{K_3} \oint_{K_4} I(s_1, \dots, s_{10}), \quad (2.5)$$

$$I(s_1, \dots, s_{10}) \equiv \frac{1}{(P_1 \cdot P_1)^{s_1} \dots (P_{10} \cdot P_{10})^{s_{10}}}, \quad (2.6)$$

where positive (negative) indices s_a correspond to propagators (numerators). Our notation distinguishes sum-integrals \mathcal{I} from their integrands I . For 4-loop contributions that factorize into lower-loop factors, it will be useful to define the 3-loop momentum family

$$\{P_1, \dots, P_6\} = \{K_1, K_2, K_3, K_{1-2}, K_{1-3}, K_{2-3}\} \quad (2.7)$$

and represent 3-loop scalar sum-integrals and their integrands as 6-element lists, in complete structural analogy to the 4-loop case.

3 Reduction to canonical form

The core of our calculation uses automatized tools as far as possible, and proceeds as follows. All Feynman diagrams are generated by **Qgraf** [40, 41] and mapped onto our preferred momentum conventions of eq. (2.4). We then use the computer algebra package **FORM** [42, 43] to plug in Feynman rules (we work in general covariant gauges with gauge parameter ξ), perform the color and Lorentz algebra, and express all resulting scalar sum-integrals in the form of lists of integers as defined in eq. (2.5). These lists are analyzed

$$\begin{aligned}
& + \frac{1}{24} \text{diagram} + \frac{1}{32} \text{diagram} + \frac{1}{48} \text{diagram} + \frac{1}{48} \text{diagram} + \frac{1}{16} \text{diagram} + \frac{1}{4} \text{diagram} + \frac{1}{16} \text{diagram} \\
& - \frac{1}{8} \text{diagram} + \frac{1}{16} \text{diagram} + \frac{1}{16} \text{diagram} - \frac{1}{8} \text{diagram} + \frac{1}{8} \text{diagram} + \frac{1}{8} \text{diagram} + \frac{1}{16} \text{diagram} \\
& + \frac{1}{24} \text{diagram} - \frac{1}{12} \text{diagram} + \frac{1}{8} \text{diagram} - \frac{1}{4} \text{diagram} - \frac{1}{2} \text{diagram} + \frac{1}{16} \text{diagram} - \frac{1}{4} \text{diagram} \\
& + \frac{1}{4} \text{diagram} + \frac{1}{8} \text{diagram} - \frac{1}{4} \text{diagram} - \frac{1}{2} \text{diagram} + \frac{1}{4} \text{diagram} - \frac{1}{2} \text{diagram} + \frac{1}{4} \text{diagram} \\
& - \frac{1}{2} \text{diagram} + \frac{1}{16} \text{diagram} - \frac{1}{8} \text{diagram} + \frac{1}{8} \text{diagram} - \frac{1}{4} \text{diagram} + \frac{1}{32} \text{diagram} - \frac{1}{8} \text{diagram} \\
& + \frac{1}{8} \text{diagram} + \frac{1}{72} \text{diagram} - \frac{1}{4} \text{diagram} - \frac{1}{6} \text{diagram} + \frac{1}{16} \text{diagram} - \frac{1}{4} \text{diagram} - \frac{1}{2} \text{diagram} \\
& - \frac{1}{2} \text{diagram} + \frac{1}{4} \text{diagram} + 1 \text{diagram} + \frac{1}{12} \text{diagram} - \frac{1}{2} \text{diagram} - \frac{1}{3} \text{diagram} - 1 \text{diagram} \\
& - \frac{1}{2} \text{diagram} + \frac{1}{6} \text{diagram} + \frac{1}{6} \text{diagram} + \frac{1}{8} \text{diagram} - \frac{1}{4} \text{diagram} - 1 \text{diagram} - \frac{1}{2} \text{diagram} - 1 \text{diagram} \\
& - \frac{1}{4} \text{diagram} + 1 \text{diagram} + \frac{1}{2} \text{diagram} + \frac{1}{48} \text{diagram} - \frac{1}{8} \text{diagram} - \frac{1}{3} \text{diagram} + \frac{1}{4} \text{diagram} - \frac{1}{6} \text{diagram}
\end{aligned}$$

Figure 3. Feynman diagrams contributing to the 4-loop pressure of pure gauge theory, $p_4(N_f = 0)$.

with `Mathematica` [44] code, which exploits the sum-integrals' invariance under linear transformations of loop momentum variables and produces replacement rules that allow to bring the lists into a canonical form. Finally, these replacement rules are applied to the sum-integrals at hand and the contributions from all diagrams are summed up, at which point we observe a very substantial reduction of terms. We will comment on some of these steps in the following section. A reader not interested in technical details might skip right ahead to eq. (3.3) where we present the form of our result.

3.1 Mapping

In practice, we start by generating all diagrams that contribute to p_4 by `Qgraf`. As a minor detail, we generate two-point functions that result from cutting a line in a (connected, one-particle irreducible) vacuum diagram and glue the two external lines back together with a propagator, correcting for the symmetry factor as explained e.g. in [11]. We perform this step in two different ways: by gluing together all (connected) gluonic⁴ self-energies, or by following the somewhat more refined procedure of [11] that consists in generating 2-particle irreducible skeleton vacuum graphs separately from 2-particle reducible ring diagrams (the relevant self-energy selection options within `Qgraf` are `onepi`, `nosigma` and `sigma`). Both

⁴Since ghosts (and quarks) do not self-interact, a vacuum diagram at two loops or higher is guaranteed to have at least one gluon propagator, such that we are guaranteed (even in full QCD) to obtain all possible vacuum diagrams from only considering gluon self-energies.

ways give rise to the set of diagrams depicted in figure 3, with precisely the same combinatorial factors, but with different internal momentum routings. We keep both sets in our computation, to provide a strong check on internal consistency and completeness of our reduction algorithm in the end of our calculation.

Suppose we are now given (by a collaborator, or a program such as `Qgraf`) a 4-loop vacuum Feynman diagram that employs a momentum list \bar{P} , not necessarily coinciding with our choice P of eq. (2.4). We then need replacement rules that map the \bar{P} onto (a subset of) the P , in order to be able to express all (sum-) integrals that arise from the given diagram in our list notation of eq. (2.5). Such replacement rules can be generated in an automatized way by comparing the so-called graph (or first Symanzik) polynomials \mathcal{U} of given momentum lists \bar{P} and P . For an L -loop graph, \mathcal{U} is a homogeneous polynomial of degree L in the variables x_a that are attached to the edges. It encodes the underlying graph in a unique way, up to re-numberings of the x_a . It plays an important role in parametric representations of Feynman integrals (see e.g. the recent textbook [45]), but we can as well make use of \mathcal{U} to detect graph isomorphisms, aided by a canonical ordering for such polynomials, based on ideas outlined in [46, 47]. Once we have detected that two graph polynomials are equivalent, we can reverse the canonical ordering to match pairs of momenta from the sets \bar{P} and P , and obtain the replacement rules. So we can guarantee that any input can be mapped onto our choice of momentum family eq. (2.4).

It is now easy to plug in the Feynman rules, perform the color and Lorentz traces (we use `FORM` for these steps) and arrive at scalar vacuum sum-integrals represented in list notation eq. (2.5). Note that we are dealing with vacuum diagrams; there are no external momenta and all (Lorentz and group) indices contract, guaranteeing a scalar (sum-) integral as outcome. Furthermore, owing to the fact that our family is complete in the sense that all scalar products $K_j^\mu K_k^\mu$ can be uniquely represented as (inverse) propagators, all structures can be represented as integrals \mathcal{I} of eq. (2.5).

Recalling eq. (2.2), the hard contribution p_4 to the bare pressure of pure $SU(N_c)$ Yang-Mills theory at order $O(g_B^6)$ follows from the 65 vacuum Feynman diagrams containing gluons and ghosts as displayed in figure 3. After applying the momentum mapping described above and in general covariant gauge, it takes the form

$$p_4(d, T) = (N_c^2 - 1) \sum_{n=1}^N \tilde{c}_n(d, \xi) \tilde{\mathcal{I}}_n(d, T), \quad (3.1)$$

where the \tilde{c}_n are polynomial coefficient functions in the dimension d and the gauge parameter ξ (where the latter occurs only up to ξ^6), and $N \sim \mathcal{O}(100000)$ is the number of distinct⁵ scalarized sum-integrals $\tilde{\mathcal{I}}_n(d, T)$ in the form of eq. (2.5), as obtained after mapping all sum-integrals produced by the complete set of diagrams onto our conventions.

⁵The exact value of N depends somewhat on how the Feynman diagrams were constructed and labelled. For example, our two different methods of generating the diagrams as explained above result in $N = 175998$ and $N = 96928$, respectively. Running both different sets through the same canonicalization algorithm and arriving at identical canonical forms can then be interpreted as a very strong check on the calculation.

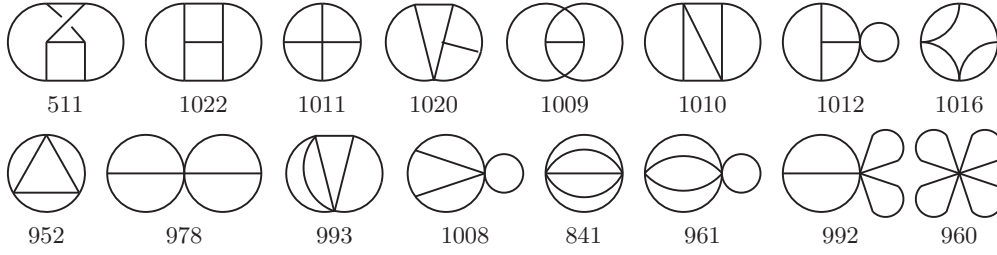


Figure 4. Set of 16 unique sector representatives for the 4-loop (sum-) integrals corresponding to the momentum family eq. (2.4). The enumeration corresponds to the decimal representation of the respective binary footprint of propagators.

3.2 Canonical form

There is enormous freedom in writing down a sum-integral. The value of \mathcal{I} does not depend on the particular propagator momentum choice. It is invariant under reparameterizations of the loop momenta. In particular, we can allow for linear changes of variables $K \rightarrow \bar{K} = SK$ where S are unimodular $L \times L$ matrices (i.e. square integer matrices with $\det S = \pm 1$). The S are clearly invertible; the transformations have unit Jacobian determinant and therefore leave the measure \mathbb{J} invariant; hence such shifts S induce equivalence relations directly among the integrands I of eq. (2.6).

We can once more make use of the graph polynomials \mathcal{U} to detect graph isomorphisms. Now, we are interested in the different ways that the same \mathcal{I} can be represented by different integrands I . Systematically applying momentum shifts S to subsets of the full family P and then comparing graphs on the basis of their canonically ordered graph polynomials \mathcal{U} as explained in section 3.1, we can define equivalence classes, and choose unique representatives. In figure 4, we display the result of such a classification on the basis of propagator lines (i.e. the positive list entries s_a of an integrand $I(s_1, \dots, s_{10})$), defining a so-called sector of the full family).

The core of our canonicalization approach can now be stated as follows: identify equivalence classes on the integrand level, pick a unique representative for each class (e.g. the “smallest” according to some ordering relation $\mathcal{I}_1 \prec \mathcal{I}_2$), and exploit the shifts S to map any (linear combination of) \mathcal{I} onto those representatives, the result of which we call the canonical form of an expression.

This concept is of course far from original, and it is indeed heavily used in perturbative quantum field theory at zero temperature, in particular in the context of algorithmic integration-by-parts (IBP) approaches [48?]. As far as we are aware, however, this machinery has not yet been systematically applied to sum-integrals on a large scale.

As can be inferred from the above, part of our strategy relies heavily on matrix operations. For ease of implementation, we have therefore opted to use a commercial computer algebra system (Wolfram Mathematica [44]) to develop key parts of our setup. We regard this choice as a proof-of-principle only, and stress that the strategy can (and maybe should) also be implemented on freely available software.

On the technical side, the large linear systems we encounter can be dealt with in an efficient way using sparse matrix representations (`SparseArray`), exact integer-matrix algorithms such as (`HermiteDecomposition`), and exploiting the block-diagonal form of the systems that is induced by the sector- and sub-sector (as obtained by deleting a line of the parent sector) structure of our sum-integrals.

3.3 Bare pressure at g^6

Let us now return to our physics problem at hand and simplify the 4-loop hard pressure of eq. (3.1). Following the strategy laid out in section 3.2, the large redundancy present in the vector space spanned by the set $\{\tilde{\mathcal{I}}_n(d, T)\}_{n=1}^N$ is alleviated upon solving a system of linear equations, generated by a systematic application of momentum shifts. In the process, we witness a significant reduction of the number of sum-integrals in need of evaluation, in addition to the explicit cancellation of all factors of ξ , serving as a non-trivial check of the correctness of the procedure. Equation (3.1) then collapses to

$$p_4(d, T) = -\frac{(N_c^2 - 1)}{72} \sum_{n=1}^{21} c_n(d) \mathcal{I}_n(d, T) \quad (3.2)$$

$$\begin{aligned} &= -\frac{(N_c^2 - 1)}{72} \left\{ (1939 - 852d + 63d^2 + 2d^3) \mathcal{I}_6 + 6(281 - 180d + 39d^2 + 4d^3) \mathcal{I}_9 \right. \\ &\quad + 2(d-1)^3 \left[9(d-9) \mathcal{I}_1 + 6(d-5) \mathcal{I}_2 + 18 \mathcal{I}_3 - 18 \mathcal{I}_4 + 12 \mathcal{I}_{10} - 48 \mathcal{I}_{11} + 27 \mathcal{I}_{12} + 36 \mathcal{I}_{13} - \mathcal{I}_{16} \right] \\ &\quad - 3(d-1)^2 \left[8(7d-31) \mathcal{I}_5 + (d+15) \mathcal{I}_{15} + 4 \mathcal{I}_{18} - 4 \mathcal{I}_{19} - 6 \mathcal{I}_{20} + 4 \mathcal{I}_{21} \right] \\ &\quad \left. + 18(41 - 19d + 2d^2) \left[\mathcal{I}_7 - 4 \mathcal{I}_8 + \mathcal{I}_{17} \right] - 18(119 - 49d + 2d^2) \mathcal{I}_{14} \right\}. \quad (3.3) \end{aligned}$$

The resulting set of 21 sum-integrals $\mathcal{I}_n(d, T)$ can be understood as a basis in the sense of corresponding to sector representatives (see figure 4) of the minimal set of integrals⁶ that are independent with respect to the graphs' internal symmetries, a property we refer to as canonical form. We enumerate and discuss the \mathcal{I}_n in the next section.

As a further check on the canonicalization procedure developed and applied for reducing the four-loop term p_4 to its compact form eq. (3.3), we can apply the same recipe for the two- and three-loop pressure, see figures 1 and 2 for the corresponding diagrams. Details and analytic d -dimensional expressions for p_0 , p_2 and p_3 of eq. (2.2) are given in appendix A. It is reassuring to observe that those expressions coincide with the known results [9, 37].

While eq. (3.3) together with the explicit \mathcal{I}_n listed in the following section is the main result of this paper, we now proceed with the characterization and evaluation of (a subset of) the \mathcal{I}_n , particularly those which are factorizable into known lower-loop factors.

4 Sum-integral evaluations

The 21 sum-integrals $\mathcal{I}_n(d, T)$ entering eq. (3.3) can be classified according to the structure of the underlying propagator graph sector. Eleven of them fall into the subset of sectors

⁶Finding a genuine linearly independent basis of so-called master integrals is only feasible after taking into account integration-by-parts relations as well. However, this is well understood only at $T = 0$ [49].

that decompose into lower-loop factors, recall figure 4 where we have displayed and labelled all such sectors. Below, we will frequently attach to each sum-integral the corresponding sector number in form of a subscript in square brackets. This is for convenience only, and does not change the basic list notation of eq. (2.5). In fact, we will also indicate the number of lines of each sector in that subscript, and omit the function arguments (d, T) for brevity.

The factorizable sum-integrals can be readily evaluated, as they are either fully known (the case of one and two loops), or can be mapped onto known 3-loop cases, thereby leaving only 10 genuine (non-factorizable) 4-loop sum-integrals in need of evaluation.

We will now turn to evaluate all 11 factorizable sum-integrals that we observe in our sum eq. (3.3), and finally list the 10 non-factorizable cases, for which we discuss possible evaluation strategies.

4.1 Factorized sectors: one loop

We obtain two sum-integrals fully factorized as four 1-loop factors, reading

$$\mathcal{I}_1 \equiv \mathcal{I}(2, 2, 1, 1, 0, 0, 0, 0, 0, 0)_{[4,960]} , \quad (4.1)$$

$$\mathcal{I}_2 \equiv \mathcal{I}(3, 1, 1, 1, 0, 0, 0, 0, 0, 0)_{[4,960]} . \quad (4.2)$$

They can be expressed in terms of the analytically known 1-loop tadpoles of eq. (B.1) as

$$\mathcal{I}_1 = (I_2^0)^2 (I_1^0)^2 , \quad \mathcal{I}_2 = I_3^0 (I_1^0)^3 . \quad (4.3)$$

4.2 Factorized sectors: two loops

Three sum-integrals factorize onto 1- and 2-loop factors; they read

$$\mathcal{I}_4 \equiv \mathcal{I}(1, 2, 1, 1, 1, 0, 0, 0, 0, 0)_{[5,992]} , \quad (4.4)$$

$$\mathcal{I}_5 \equiv \mathcal{I}(2, 1, 1, 1, 1, 0, 0, 0, 0, 0)_{[5,992]} , \quad (4.5)$$

$$\mathcal{I}_7 \equiv \mathcal{I}(1, 1, 1, 1, 0, 1, 0, 0, 1, 0)_{[6,978]} . \quad (4.6)$$

Using eqs. (B.1) and (B.3), they can be written as

$$\mathcal{I}_4 = L_{1,1,1}^{0,0,0} I_1^0 I_2^0 , \quad \mathcal{I}_5 = L_{2,1,1}^{0,0,0} (I_1^0)^2 , \quad \mathcal{I}_7 = (L_{1,1,1}^{0,0,0})^2 . \quad (4.7)$$

Applying the generic reduction formula of [50] to the 2-loop factors L then results in

$$\mathcal{I}_4 = 0 , \quad \mathcal{I}_5 = -\frac{(I_1^0)^2 (I_2^0)^2}{(d-5)(d-2)} , \quad \mathcal{I}_7 = 0 . \quad (4.8)$$

4.3 Factorizable sectors: three loops

Six of our sum-integrals are built from one 1-loop and one 3-loop structure, and we have in fact already discussed these cases earlier [51]. They are

$$\mathcal{I}_3 \equiv \mathcal{I}(2, 1, 1, 1, 0, 0, 0, 0, 0, 1)_{[5,961]} , \quad (4.9)$$

$$\mathcal{I}_9 \equiv \mathcal{I}(1, 1, 1, 1, 1, 1, 0, 0, 0, 0)_{[6,1008]} , \quad (4.10)$$

$$\mathcal{I}_{10} \equiv \mathcal{I}(1, 1, 1, 3, 1, 1, 0, 0, -2, 0)_{[6,1008]} , \quad (4.11)$$

$$\mathcal{I}_{11} \equiv \mathcal{I}(1, 1, 1, 3, 1, 1, 0, 0, -1, -1)_{[6,1008]} , \quad (4.12)$$

$$\mathcal{I}_{12} \equiv \mathcal{I}(1, 1, 1, 3, 1, 1, 0, 0, 0, -2)_{[6,1008]} , \quad (4.13)$$

$$\mathcal{I}_{13} \equiv \mathcal{I}(2, 1, 1, 2, 1, 1, 0, -1, 0, -1)_{[6,1008]} . \quad (4.14)$$

Note that sector [1012] does not contribute. The sum-integrals \mathcal{I}_3 and \mathcal{I}_9 do not have numerators and trivially decouple into two factors. In terms of the known 3-loop cases given in eqs. (B.7) and (B.10), they evaluate to

$$\mathcal{I}_3 = J_1 I_1^0, \quad \mathcal{I}_9 = J_{11} I_1^0. \quad (4.15)$$

The four remaining sum-integrals of eqs. (4.11)–(4.14) contain numerator factors, necessitating tensor decomposition in order to decouple their 1- and 3-loop parts. Thanks to the presence of the 1-loop tadpole factor this is straightforward, and we can apply the general method developed in [51]. After furthermore employing simple 3-loop IBP reductions as well as the 2-loop reduction formula of [50], this leads to [51]

$$\mathcal{I}_{10} = \frac{16}{d(d-2)(d-7)} I_1^2 I_3^0 I_2^0 I_1^0 - \frac{(I_2^0)^2 (I_1^0)^2}{(d-2)(d-5)} + \frac{4(d+1)}{d} V_4 I_1^2, \quad (4.16)$$

$$\begin{aligned} \mathcal{I}_{11} = & I_3^0 (I_1^0)^3 + \frac{16}{d(d-2)(d-7)} I_1^2 I_3^0 I_2^0 I_1^0 + \frac{(d+1)}{d(d-2)(d-5)^2} I_1^2 (I_2^0)^3 \\ & + \frac{(d+1)}{d(d-5)} V_1 I_1^2 - \frac{(4-7d+d^2)}{2d(d-5)} V_2 I_1^2 + \frac{4(d+1)}{d} V_4 I_1^2, \end{aligned} \quad (4.17)$$

$$\begin{aligned} \mathcal{I}_{12} = & J_{13} I_1^0 + \frac{32}{d(d-2)(d-7)} I_1^2 I_3^0 I_2^0 I_1^0 + \frac{2(d+1)}{d(d-2)(d-5)^2} I_1^2 (I_2^0)^3 \\ & + \frac{2(d+1)}{d(d-5)} V_1 I_1^2 - \frac{(4-7d+d^2)}{d(d-5)} V_2 I_1^2 + \frac{8(d+1)}{d} V_4 I_1^2, \end{aligned} \quad (4.18)$$

$$\mathcal{I}_{13} = \frac{1}{2} I_1^0 \left[\frac{2(2d-11)}{(d-5)} (I_2^0)^2 I_1^0 - J_1 - 2 J_{11} - 4(d-4) J_{12} \right]. \quad (4.19)$$

All the required 3-loop sum-integrals are known up to $O(\varepsilon^0)$, and listed in appendix B.3.

4.4 Non-factorized sectors

The ten remaining sum-integrals fall in the category of genuine non-factorized sectors, and none of them is known (except for \mathcal{I}_6 ; see below). They read

$$\mathcal{I}_6 \equiv \mathcal{I}(1, 1, 1, 0, 1, 1, 1, 0, 0, 0)_{[6,952]}, \quad (4.20)$$

$$\mathcal{I}_8 \equiv \mathcal{I}(1, 1, 1, 1, 1, 0, 0, 0, 0, 1)_{[6,993]}, \quad (4.21)$$

$$\mathcal{I}_{14} \equiv \mathcal{I}(1, 1, 1, 1, 1, 1, 0, 0, -1, 1)_{[7,1009]}, \quad (4.22)$$

$$\mathcal{I}_{15} \equiv \mathcal{I}(1, 1, 1, 2, 1, 1, 1, 0, 0, -2)_{[7,1016]}, \quad (4.23)$$

$$\mathcal{I}_{16} \equiv \mathcal{I}(1, 1, 1, 3, 1, 1, 1, 0, 0, -3)_{[7,1016]}, \quad (4.24)$$

$$\mathcal{I}_{17} \equiv \mathcal{I}(1, 1, 1, 1, 1, 1, -1, -1, 1, 1)_{[8,1011]}, \quad (4.25)$$

$$\mathcal{I}_{18} \equiv \mathcal{I}(1, 1, 1, 1, 1, 1, 0, -2, 1, 1)_{[8,1011]}, \quad (4.26)$$

$$\mathcal{I}_{19} \equiv \mathcal{I}(1, 1, 1, 1, 1, 1, 1, 1, -2, 0)_{[8,1020]}, \quad (4.27)$$

$$\mathcal{I}_{20} \equiv \mathcal{I}(1, 1, 1, 1, 1, 1, 1, 1, 0, -2)_{[8,1020]}, \quad (4.28)$$

$$\mathcal{I}_{21} \equiv \mathcal{I}(1, 1, 1, 1, 1, 1, 1, 1, 1, -3)_{[9,1022]}. \quad (4.29)$$

Note that sectors [841], [1010] and the non-planar [511] are not present.⁷ Within the family of 4-loop non-factorized sectors, we can identify three separate subcategories \mathcal{S}_i based on the types of subgraphs these graphs are built from, suggesting in this way a hierarchy of complexity in their evaluation.

First, the subset $\mathcal{S}_1 = \{\mathcal{I}_6, \mathcal{I}_{15}, \mathcal{I}_{16}\}$ contains members of sectors [952] and [1016], made up of three simple 1-loop 2-point subgraphs. The machinery for tackling such types of vacuum graphs was developed in [24], relying on systematic subtractions of divergences present in the subgraphs, essentially mapping the problem to a numerical finite contribution plus a divergent lower-loop piece. Up to three loops, a number of sum-integrals (given in appendix B.3) have been evaluated using this method. Similarly, the only 4-loop bosonic vacuum sum-integral that has ever been computed [52] belongs to sector [952] and heavily relied on this approach as well. Concretely, in [52] a specific linear combination of sum-integrals had been evaluated, see our appendix B.4 for the detailed form. The motivation for considering that linear combination had come from including terms that arise from lower loop orders when renormalizing the coupling constant of the scalar theory considered in [52]. In practice, this helped cancelling logarithmic ultraviolet divergences present in the 1-loop 2-point subgraphs. In terms of the (UV-subtracted) 4-loop sum-integral S_2 evaluated in [52] and given in appendix B.4, we can at least rewrite

$$\mathcal{I}_6 = \Lambda^{-8\varepsilon} S_2 + \frac{3}{\varepsilon} \left[\lim_{\varepsilon \rightarrow 0} \varepsilon I_2^0 \right] B_2 . \quad (4.30)$$

Here, B_2 is a 3-loop basketball-type sum-integral from appendix B.3, whose $\mathcal{O}(\varepsilon)$ term that would be required to expand \mathcal{I}_6 up to the constant term is currently unknown, however. The term in square brackets is finite; it extracts the coefficient of the prototype divergence of one-loop sum-integrals (see appendix B.1) and equals $(4\pi)^{-2}$.

The two sum-integrals within sector [1016] in \mathcal{S}_1 , in contrast, contain non-trivial numerators. In analogy to the procedure carried out in section 4.3, these can be mapped onto (partially) known structures upon tensor decomposition of 1-loop 2-point functions, slightly generalizing the 1-loop tadpole decomposition formulae of [51]. We obtain

$$\mathcal{I}_{15} = 12 \tilde{\mathcal{I}}_{15} - 3 \mathcal{I}_9 - \frac{1}{2} \mathcal{I}_6 + 6 \mathcal{I}_5 , \quad (4.31)$$

$$\mathcal{I}_{16} = 48 \tilde{\mathcal{I}}_{16} - \frac{3}{2} \mathcal{I}_{15} + 9 \mathcal{I}_{12} - 12 \mathcal{I}_{11} + 12 \mathcal{I}_{10} - 6 \mathcal{I}_9 - \frac{1}{2} \mathcal{I}_6 + 24 \mathcal{I}_5 , \quad (4.32)$$

where on the right-hand side we encounter factorized 4-loop sum-integrals evaluated in sections 4.2 and 4.3, as well as two new 4-loop sum-integrals that contain explicit 1-loop tensor 2-point functions

$$\tilde{\mathcal{I}}_{15} \equiv \oint_K \Pi(K) \Pi^{\mu\nu}(K) \Pi^{\mu\nu}(K) , \quad \tilde{\mathcal{I}}_{16} \equiv \oint_K \Pi^{\mu\nu}(K) \Pi^{\nu\rho}(K) \Pi^{\rho\mu}(K) , \quad (4.33)$$

$$\text{with } \Pi(K) \equiv \oint_Q \frac{1}{Q^2 (Q-K)^2} , \quad \Pi^{\mu\nu}(K) \equiv \frac{1}{K^2} \oint_Q \frac{Q^\mu Q^\nu}{Q^2 (Q-K)^2} , \quad (4.34)$$

⁷Remarkably, all non-planar vacuum Feynman diagrams in Yang-Mills theory at four loops vanish identically after performing the color trace over the totally antisymmetric structure constants f^{abc} .

and still need to be evaluated. To this end, we observe that a similar mapping had already been performed when evaluating the 3-loop sum-integrals B_3 and J_{13} of appendix B.3, where tensor structures of this form were dealt with using a general decomposition method based on dimensional shifts, followed by the standard subtraction of divergences of the 1-loop subgraphs [53]. While one still expects such a strategy to be applicable in eq. (4.33), the presence of an additional Π -insertion as compared to the 3-loop counterpart significantly increases the number of subtraction terms, in addition to the possible appearance of various divergences of the form

$$\frac{1}{\varepsilon} \not\int_K \frac{1}{[K^2]^s} \Pi(K) \Pi(K) \quad (4.35)$$

that had already affected the direct evaluation of \mathcal{I}_6 discussed above. This could motivate the search for completely new evaluation methods altogether, going beyond the proven 1-loop subtraction strategies.

Second, the subset $\mathcal{S}_2 = \{\mathcal{I}_8, \mathcal{I}_{14}, \mathcal{I}_{19}, \mathcal{I}_{20}\}$ has one member in sector [993], one in [1009] and two in [1020]. These consist of insertions of 1-loop and 2-loop 2-point subgraphs, the latter of which requires a generalization of the 1-loop sub-divergence subtraction strategy. Within this set, \mathcal{I}_8 might be a nice starting point as it does not contain numerators.

Third, the final subset $\mathcal{S}_3 = \{\mathcal{I}_{17}, \mathcal{I}_{18}, \mathcal{I}_{21}\}$ consists of two sum-integrals falling into sector [1011] and one in [1022]. Their structure appears the most intricate of our list, being made up from two subgraphs with 3-point structure, for which there does not seem to exist previous experience regarding evaluation methods.

5 Conclusions

We have reported on major progress towards solving a long-standing open problem in finite-temperature field theory. The last missing piece in an effective theory approach as sketched in [9] and applied to evade an infrared problem that concerns the QCD pressure has been reduced into what now seems a manageable form. To do so, we have confronted the open 4-loop strict perturbative expansion of the hard-mode contributions to the pressure, summing up the 65 Feynman diagrams shown in figure 3 and manipulating the corresponding sum-integrals with modern algorithmic methods.

Bringing the integrand into canonical form has enabled us to reduce the number of Feynman sum-integrals that contribute to the four-loop pressure of hot $SU(N_c)$ gauge theory from order 10^5 down to 21, at the same time obtaining explicit gauge-parameter independence. Furthermore, we have linked the evaluations of 11 of these 21 remaining masters to previously known results, such that only 10 genuine 4-loop sum-integrals remain to be considered, as listed in eqs. (4.20)–(4.29). The evaluation of which, up to the constant term in the ε -expansion, we leave as an exercise for the reader.

Once the ten remaining 4-loop sum-integrals are available, it will be a most enjoyable task to collect all ingredients of the effective theory setup and put them together for the long sought-after “physical leading-order” result for the hot Yang-Mills pressure, and to present an update on issues such as series convergence, (renormalization) scale dependence and a parameter-free comparison to lattice data.

Looking forward, a generalization of our canonical approach to include quarks is not difficult, as they do not self-interact and hence only occur in closed loops. Therefore, one merely needs to keep track of the fermion signature of the four loop momenta K_j when performing momentum shifts, and we expect similarly spectacular reductions for unintegrated expressions in full thermal QCD at four loops as those observed here for the $N_f = 0$ case. Furthermore, the setup can then be easily extended to the case of dense QCD by keeping track of signs of propagator momenta [54].

Finally, we anticipate that it might even be feasible to compute a correction to the full 4-loop pressure. Indeed the next term in the effective field theory setup is of order g^7 and entails a five-loop computation within 3-dimensional gauge theory coupled to a massive scalar (known as EQCD in the literature). Technically, this corresponds to regular (zero-temperature) continuum vacuum Feynman integrals of QED-type, which coincidentally are currently being studied [56] in the collider physics community.

Acknowledgments

P.N. has been supported by an ANID grant Magíster Nacional No. 22211544, by the Doctoral School of the University of Helsinki, and by the Academy of Finland grants No. 347499, 353772 and 1322507. Y.S. acknowledges support from ANID under FONDECYT projects No. 1191073 and 1231056, and from UBB/VRIP project No. EQ2351247. All figures have been prepared with Axodraw [55].

A Bare pressure up to g^4

As a further check on the canonicalization procedure developed and applied for reducing the four-loop term p_4 to its compact form eq. (3.3), we can apply the same recipe for the two- and three-loop pressure.

We again start with two different strategies to generate the diagrams as explained in section 3.1, obtaining the sets shown in figures 1 and 2. Next, we re-run the same classification, scalarization and canonicalization algorithm of section 3.2 over the sum-integrals corresponding to those diagrams. Adding the d -dimensional form of the leading-order term (for a recent textbook see [57]), we obtain the coefficients of eq. (2.2) (at $N_f = 0$)

$$p_0(d, T) = -(N_c^2 - 1) \frac{d-1}{2} \oint_K \ln(K^2), \quad (\text{A.1})$$

$$p_2(d, T) = -(N_c^2 - 1) \frac{(d-1)^2}{4} \oint_K \oint_Q \frac{1}{K^2 Q^2}, \quad (\text{A.2})$$

$$p_3(d, T) = (N_c^2 - 1) \frac{(d-1)^2}{8} \left[2(d-5) \mathcal{I}(2, 1, 1, 0, 0, 0) + \mathcal{I}(1, 1, 0, 0, 1, 1) \right. \\ \left. - 4 \mathcal{I}(1, 1, 1, 1, 0, 0) + 2 \mathcal{I}(2, 1, 1, 1, 1, -2) \right], \quad (\text{A.3})$$

where for the 3-loop pressure our algorithm has employed the corresponding 6-element momentum family eq. (2.7).

Finally, we follow the strategy of section 4 and identify factorizable sectors, which in this case do not have numerators and decompose trivially into 1-loop factors I_ν^η of appendix B.1. For the remaining sum-integrals in p_3 we use the naming scheme of appendix B.2 and B.3 which results in

$$p_0(d, T) = -(N_c^2 - 1) \frac{d-1}{d} I_1^2, \quad (\text{A.4})$$

$$p_2(d, T) = -(N_c^2 - 1) \frac{(d-1)^2}{4} (I_1^0)^2, \quad (\text{A.5})$$

$$p_3(d, T) = (N_c^2 - 1) \frac{(d-1)^2}{8} \left[2(d-5) I_2^0 (I_1^0)^2 + B_2 - 4 L_{1,1,1}^{0,0,0} I_1^0 + 2 B_3 \right]. \quad (\text{A.6})$$

Note that the two-loop sum-integral $L_{1,1,1}^{0,0,0} = 0$ (cf. eq. (4.8)) could be dropped from the last line. These expressions coincide with the known results, see e.g. [9, 37], and should come in handy when passing from the bare to the renormalized pressure.

B Massless bosonic vacuum sum-integrals

Here, we collect known results for scalar massless bosonic vacuum sum-integrals up to the four-loop level. Starting at two loops, we refrain from displaying the explicit expressions, but rather point to the original references where those results can be found.

One technical detail that was not needed in the main text but is relevant here is the following. The presence of a heat bath breaks Lorentz invariance down to just rotations in three-dimensional Euclidean space, introducing a four-vector $U = (1, \mathbf{0})$ on which tensor structures may depend. As a consequence, powers of $U^\mu K^\mu \equiv U \cdot K = K_0$ can appear in the numerators of sum-integrals. We keep track of such numerator powers wherever required by simply adding four more list entries in eq. (2.4) (three in eq. (2.7)). All techniques explained in the main text, such as sector classification, momentum shifts, or canonicalization of the sum-integrals apply to such augmented index lists as well.

B.1 One loop

The most general scalar 1-loop massless bosonic vacuum sum-integral can be computed analytically in d dimensions ($\eta \in \mathbb{N}_0$ and $\nu \in \mathbb{Z}$):

$$I_\nu^\eta(d, T) \equiv \oint_K \frac{(K_0)^\eta}{[K^2]^\nu} = \frac{[1 + (-1)^\eta] T \zeta(2\nu - \eta - d)}{(2\pi T)^{2\nu - \eta - d}} \frac{\Gamma(\nu - \frac{d}{2})}{(4\pi)^{d/2} \Gamma(\nu)}. \quad (\text{B.1})$$

Note that I_ν^η vanishes for odd values of η as a consequence of the integrand's symmetry under $K_0 \rightarrow -K_0$.

Another “one-loop” case of interest is the type of sum-integral that enters the ideal gas pressure, arising from the logarithms of a Gaussian path integral over the quadratic part of the action. From dimensional analysis and taking a derivative with respect to the temperature, it can be related [37] to the integrals of eq. (B.1) as

$$\oint_K \ln(K^2) = \frac{2}{d} I_1^2(d, T) \stackrel{d=3-2\varepsilon}{\approx} -\frac{\pi^2 T^4}{45} + \mathcal{O}(\varepsilon). \quad (\text{B.2})$$

B.2 Two loops

The most general scalar 2-loop massless bosonic vacuum sum-integral has the form

$$L_{\nu_1, \nu_2, \nu_3}^{\eta_1, \eta_2, \eta_3}(d, T) \equiv \oint_K \oint_Q \frac{(K_0)^{\eta_1} (Q_0)^{\eta_2} (K_0 - Q_0)^{\eta_3}}{[K^2]^{\nu_1} [Q^2]^{\nu_2} [(K - Q)^2]^{\nu_3}}. \quad (\text{B.3})$$

It turns out that for any combination of indices $\eta_i \in \mathbb{N}_0$ and $\nu_i \in \mathbb{Z}$, $L_{\nu_1, \nu_2, \nu_3}^{\eta_1, \eta_2, \eta_3}$ reduces to a sum of products of two 1-loop tadpoles I_ν^η , as given in eq. (B.1). This reduction is a consequence of integration-by-parts (IBP) identities that can either be applied at fixed integer values of $\{\eta_i, \nu_j\}$ [37], or even solved for the general case [58], leading to an explicit closed formula for the reduction $L \rightarrow I \times I$ in the general-index case [50].

B.3 Three loops

At the 3-loop level, all available results have been obtained only up to the constant term in the ε expansion in dimensional regularization, making use of the methods pioneered by Arnold and Zhai [24]. In the following, we employ the 3-loop propagator momentum family $\{P_a\}$ defined in eq. (2.7) and add three additional indices to our index-list to account for factors of Matsubara frequencies in the numerators. The general vacuum sum-integral can then be represented in our list-notation as (recall $U = (1, \mathbf{0})$)

$$\oint_{K_1} \oint_{K_2} \oint_{K_3} \frac{(U \cdot K_1)^{m_1} (U \cdot K_2)^{m_2} (U \cdot K_3)^{m_3}}{(P_1 \cdot P_1)^{s_1} \dots (P_6 \cdot P_6)^{s_6}} \equiv \mathcal{I}(s_1, \dots, s_6; m_1, \dots, m_3). \quad (\text{B.4})$$

At mass dimension 4 (relevant the 3-loop pressure), the following sum-integrals are known (see [37] for an overview)

$$B_2 = \mathcal{I}(1, 1, 0, 0, 1, 1; 0, 0, 0) \quad (I_{\text{ball}} \text{ in [24]; } \mathcal{M}_{0,0} \text{ in [59]}), \quad (\text{B.5})$$

$$B_3 = \mathcal{I}(2, 1, 1, 1, 1, -2; 0, 0, 0) \quad (\text{related to } I_{\text{sqed}} \text{ in [24]; } \mathcal{M}_{2,-2} \text{ in [59]}). \quad (\text{B.6})$$

At mass dimension 2 (relevant for the matching parameter m_E^2 in EQCD), the following sum-integrals are known (see [19] for an overview)

$$J_{11} = \mathcal{I}(1, 1, 1, 1, 1, 0; 0, 0, 0) \quad (I \text{ in [60]; } \mathcal{M}_{1,0} \text{ in [59]}), \quad (\text{B.7})$$

$$J_{12} = \mathcal{I}(2, 1, 1, 1, 1, 0; 0, 2, 0) \quad (V_2 \text{ in [61]}), \quad (\text{B.8})$$

$$J_{13} = \mathcal{I}(3, 1, 1, 1, 1, -2; 0, 0, 0) \quad (\mathcal{M}_{3,-2} \text{ in [53]}), \quad (\text{B.9})$$

$$J_1 = \mathcal{I}(2, 1, 0, 0, 1, 1; 0, 0, 0) \quad (S_1 \text{ in [52]; } B_2 \text{ in [62]}), \quad (\text{B.10})$$

$$J_4 = \mathcal{I}(3, 1, 0, 0, 1, 1; 2, 0, 0) \quad (B_{3,2} \text{ in [63]}). \quad (\text{B.11})$$

We note that these integrals are not all independent, since one can derive a linear relation between three of them via IBP methods (see appendix B of [63]),

$$0 = 3(d-3)^2(d-4) J_{11} - 2(3d^2 - 24d + 47) J_1 - 16(d-4) J_4. \quad (\text{B.12})$$

At mass dimension 0 (relevant for the effective coupling g_E^2 in EQCD), the following sum-integrals are known (see [64] for an overview)

$$V_1 = \mathcal{I}(1, 2, 1, 1, 1, 0; 0, 0, 0) \quad (V_1 \text{ in [65]}) , \quad (\text{B.13})$$

$$V_2 = \mathcal{I}(2, 1, 1, 1, 1, 0; 0, 0, 0) \quad (V(3; 21111; 000) \text{ in [64]}) , \quad (\text{B.14})$$

$$V_3 = \mathcal{I}(2, 2, 1, 1, 1, 0; 0, 0, 2) \quad (V(3; 22111; 002) \text{ in [64]}) , \quad (\text{B.15})$$

$$V_4 = \mathcal{I}(3, 1, 1, 1, 1, 0; 0, 2, 0) \quad (V(3; 31111; 020) \text{ in [64]}) , \quad (\text{B.16})$$

$$V_5 = \mathcal{I}(4, 1, 1, 1, 1, 0; 0, 2, 2) \quad (V(3; 41111; 022) \text{ in [64]}) , \quad (\text{B.17})$$

$$V_6 = \mathcal{I}(3, 1, 0, 0, 1, 1; 0, 0, 0) \quad (B_3 \text{ in [62]}) . \quad (\text{B.18})$$

Of these, only V_1 , V_2 and V_4 are needed for our factorizations of section 4.3.

B.4 Four loops

To date, a single genuine (ultraviolet-subtracted, bosonic) 4-loop sum-integral has been evaluated. It is the only sum-integral at the 4-loop level contributing to the (renormalized) pressure of massless scalar ϕ^4 theory. Using the scalar 1-loop two-point sum-integral

$$\Pi(K) = \oint_Q \frac{1}{Q^2(K-Q)^2} , \quad (\text{B.19})$$

the 4-loop sum-integral that has been evaluated in [52] reads

$$S_2 \equiv \Lambda^{8\epsilon} \oint_K \left([\Pi(K)]^3 - \frac{3\Lambda^{-2\epsilon}}{(4\pi)^2\epsilon} [\Pi(K)]^2 \right) \approx -\frac{T^4}{(4\pi)^4} \frac{1}{16\epsilon^2} \left(1 + \epsilon t_{11} + \epsilon^2 t_{12} \right) + \mathcal{O}(\epsilon) . (\text{B.20})$$

Here, t_{11} is a fully analytic coefficient and t_{12} is numerical. The subtraction term appearing in eq. (B.20) originates from gauge coupling renormalization in the above-mentioned theory. The inclusion of this counterterm significantly simplifies the computation of this sum-integral, as one avoids the need to evaluate a three-loop sum-integral up to $\mathcal{O}(\epsilon)$, a feat that goes beyond current sum-integral technology.

References

- [1] A. D. Linde, *Phase Transitions in Gauge Theories and Cosmology*, Rept. Prog. Phys. **42** (1979), 389.
- [2] A. D. Linde, *Infrared Problem in Thermodynamics of the Yang-Mills Gas*, Phys. Lett. B **96** (1980), 289-292.
- [3] D. J. Gross, R. D. Pisarski and L. G. Yaffe, *QCD and Instantons at Finite Temperature*, Rev. Mod. Phys. **53** (1981), 43.
- [4] N. P. Landsman, *Limitations to Dimensional Reduction at High Temperature*, Nucl. Phys. B **322** (1989), 498-530.
- [5] J. P. Blaizot and E. Iancu, *The Quark gluon plasma: Collective dynamics and hard thermal loops*, Phys. Rept. **359** (2002), 355-528 [arXiv:hep-ph/0101103].
- [6] P. H. Ginsparg, *First Order and Second Order Phase Transitions in Gauge Theories at Finite Temperature*, Nucl. Phys. B **170** (1980), 388-408.

- [7] T. Appelquist and R. D. Pisarski, *High-Temperature Yang-Mills Theories and Three-Dimensional Quantum Chromodynamics*, Phys. Rev. D **23** (1981), 2305.
- [8] K. Kajantie, M. Laine, K. Rummukainen and M. E. Shaposhnikov, *Generic rules for high temperature dimensional reduction and their application to the standard model*, Nucl. Phys. B **458** (1996), 90-136 [arXiv:hep-ph/9508379].
- [9] E. Braaten and A. Nieto, *Free energy of QCD at high temperature*, Phys. Rev. D **53** (1996), 3421-3437 [arXiv:hep-ph/9510408].
- [10] K. Kajantie, M. Laine, K. Rummukainen and Y. Schröder, *How to resum long distance contributions to the QCD pressure?*, Phys. Rev. Lett. **86** (2001), 10-13 [arXiv:hep-ph/0007109].
- [11] K. Kajantie, M. Laine and Y. Schröder, *A Simple way to generate high order vacuum graphs*, Phys. Rev. D **65** (2002), 045008 [arXiv:hep-ph/0109100].
- [12] K. Kajantie, M. Laine, K. Rummukainen and Y. Schröder, *Four loop vacuum energy density of the $SU(N_c) +$ adjoint Higgs theory*, JHEP **04** (2003), 036 [arXiv:hep-ph/0304048].
- [13] A. Hietanen, K. Kajantie, M. Laine, K. Rummukainen and Y. Schröder, *Plaquette expectation value and gluon condensate in three dimensions*, JHEP **01** (2005), 013 [arXiv:hep-lat/0412008].
- [14] P. Giovannangeli, *Two loop renormalization of the magnetic coupling and non-perturbative sector in hot QCD*, Nucl. Phys. B **738** (2006), 23-47 [arXiv:hep-ph/0506318].
- [15] Y. Schröder and M. Laine, *Spatial string tension revisited*, PoS **LAT2005** (2006), 180 [arXiv:hep-lat/0509104].
- [16] F. Di Renzo, M. Laine, V. Miccio, Y. Schröder and C. Torrero, *The Leading non-perturbative coefficient in the weak-coupling expansion of hot QCD pressure*, JHEP **07** (2006), 026 [arXiv:hep-ph/0605042].
- [17] F. Di Renzo, M. Laine, Y. Schröder and C. Torrero, *Four-loop lattice-regularized vacuum energy density of the three-dimensional $SU(3) +$ adjoint Higgs theory*, JHEP **09** (2008), 061 [arXiv:0808.0557].
- [18] M. Laine and Y. Schröder, *Quark mass thresholds in QCD thermodynamics*, Phys. Rev. D **73** (2006), 085009 [arXiv:hep-ph/0603048].
- [19] I. Ghisoiu, J. Möller and Y. Schröder, *Debye screening mass of hot Yang-Mills theory to three-loop order*, JHEP **11** (2015), 121 [arXiv:1509.08727].
- [20] E. V. Shuryak, *Theory of Hadronic Plasma*, Sov. Phys. JETP **47** (1978), 212-219.
- [21] S. A. Chin, *Transition to Hot Quark Matter in Relativistic Heavy Ion Collision*, Phys. Lett. B **78** (1978), 552-555.
- [22] J. I. Kapusta, *Quantum Chromodynamics at High Temperature*, Nucl. Phys. B **148** (1979), 461-498.
- [23] T. Toimela, *The Next Term in the Thermodynamic Potential of QCD*, Phys. Lett. B **124** (1983), 407-409.
- [24] P. B. Arnold and C. X. Zhai, *The Three loop free energy for pure gauge QCD*, Phys. Rev. D **50** (1994), 7603-7623 [arXiv:hep-ph/9408276].
- [25] P. B. Arnold and C. X. Zhai, *The Three loop free energy for high temperature QED and QCD with fermions*, Phys. Rev. D **51** (1995), 1906-1918 [arXiv:hep-ph/9410360].

- [26] C. X. Zhai and B. M. Kastening, *The Free energy of hot gauge theories with fermions through g^5* , Phys. Rev. D **52** (1995), 7232-7246 [arXiv:hep-ph/9507380].
- [27] A. Gynther, A. Kurkela and A. Vuorinen, *The $N_f^3 g^6$ term in the pressure of hot QCD*, Phys. Rev. D **80** (2009), 096002 [arXiv:0909.3521].
- [28] K. Kajantie, M. Laine, K. Rummukainen and M. E. Shaposhnikov, *3-D $SU(N)$ + adjoint Higgs theory and finite temperature QCD*, Nucl. Phys. B **503** (1997), 357-384 [arXiv:hep-ph/9704416].
- [29] J. P. Blaizot, E. Iancu and A. Rebhan, *On the apparent convergence of perturbative QCD at high temperature*, Phys. Rev. D **68** (2003), 025011 [arXiv:hep-ph/0303045].
- [30] K. Kajantie, M. Laine, K. Rummukainen and Y. Schröder, *The Pressure of hot QCD up to $g^6 \ln(1/g)$* , Phys. Rev. D **67** (2003), 105008 [arXiv:hep-ph/0211321].
- [31] Y. Schröder, *Weak-coupling expansion of the hot QCD pressure*, PoS **JHW2005** (2006), 029 [arXiv:hep-ph/0605057].
- [32] G. Boyd, J. Engels, F. Karsch, E. Laermann, C. Legeland, M. Lütgemeier and B. Petersson, *Thermodynamics of $SU(3)$ lattice gauge theory*, Nucl. Phys. B **469** (1996), 419-444 [arXiv:hep-lat/9602007].
- [33] B. Beinlich, F. Karsch, E. Laermann and A. Peikert, *String tension and thermodynamics with tree level and tadpole improved actions*, Eur. Phys. J. C **6** (1999), 133-140 [arXiv:hep-lat/9707023].
- [34] M. Okamoto *et al.* [CP-PACS], *Equation of state for pure $SU(3)$ gauge theory with renormalization group improved action*, Phys. Rev. D **60** (1999), 094510 [arXiv:hep-lat/9905005].
- [35] S. Borsanyi, G. Endrodi, Z. Fodor, S. D. Katz and K. K. Szabo, *Precision $SU(3)$ lattice thermodynamics for a large temperature range*, JHEP **07** (2012), 056 [arXiv:1204.6184].
- [36] N. P. Landsman and C. G. van Weert, *Real and Imaginary Time Field Theory at Finite Temperature and Density*, Phys. Rept. **145** (1987), 141.
- [37] M. Nishimura and Y. Schröder, *IBP methods at finite temperature*, JHEP **09** (2012), 051 [arXiv:1207.4042].
- [38] G. D. Moore, *Pressure of hot QCD at large N_f* , JHEP **10** (2002), 055 [arXiv:hep-ph/0209190].
- [39] A. Ipp, G. D. Moore and A. Rebhan, *Comment on and erratum to ‘Pressure of hot QCD at large N_f ’*, JHEP **01** (2003), 037 [arXiv:hep-ph/0301057].
- [40] P. Nogueira, *Automatic Feynman Graph Generation*, J. Comput. Phys. **105** (1993), 279-289.
- [41] P. Nogueira, *Abusing QGRAF*, Nucl. Instrum. Meth. A **559** (2006), 220-223.
- [42] J. A. M. Vermaseren, *New features of FORM*, [arXiv:math-ph/0010025].
- [43] T. Ueda, T. Kaneko, B. Ruijl and J. A. M. Vermaseren, *Further developments of FORM*, J. Phys. Conf. Ser. **1525** (2020), 012013.
- [44] Wolfram Research, Inc., *Mathematica, Version 14.1*, Champaign, IL (2024).
- [45] S. Weinzierl, *Feynman Integrals. A Comprehensive Treatment for Students and Researchers*, Springer, 2022, [arXiv:2201.03593].

- [46] A. Pak, *The toolbox of modern multi-loop calculations: novel analytic and semi-analytic techniques*, J. Phys. Conf. Ser. **368** (2012), 012049 [arXiv:1111.0868].
- [47] J. S. Hoff, *Methods for multiloop calculations and Higgs boson production at the LHC*, PhD thesis, KIT Karlsruhe (2015).
- [48] K. G. Chetyrkin and F. V. Tkachov, *Integration by parts: The algorithm to calculate β -functions in 4 loops*, Nucl. Phys. B **192** (1981), 159-204.
bibitemLaporta:2000dsw S. Laporta, *High-precision calculation of multiloop Feynman integrals by difference equations* Int. J. Mod. Phys. A **15** (2000), 5087-5159 [arXiv:hep-ph/0102033].
- [49] A. V. Smirnov and A. V. Petukhov, *The Number of Master Integrals is Finite*, Lett. Math. Phys. **97** (2011), 37-44 [arXiv:1004.4199].
- [50] A. I. Davydychev, P. Navarrete and Y. Schröder, *Factorizing two-loop vacuum sum-integrals*, JHEP **02** (2024), 104 [arXiv:2312.17367].
- [51] P. Navarrete and Y. Schröder, *Tackling the infamous g^6 term of the QCD pressure*, PoS **LL2022** (2022), 014 [arXiv:2207.10151].
- [52] A. Gynther, M. Laine, Y. Schröder, C. Torrero and A. Vuorinen, *Four-loop pressure of massless $O(N)$ scalar field theory*, JHEP **04** (2007), 094 [arXiv:hep-ph/0703307].
- [53] I. Ghisoiu and Y. Schröder, *A New Method for Taming Tensor Sum-Integrals*, JHEP **11** (2012), 010 [arXiv:1208.0284].
- [54] P. Navarrete, R. Paaelainen and K. Seppänen, *Perturbative QCD meets phase quenching: The pressure of cold quark matter*, [arXiv:2403.02180].
- [55] J. C. Collins and J. A. M. Vermaseren, *Axodraw Version 2*, [arXiv:1606.01177].
- [56] A. Maier, P. Marquard and Y. Schröder, *Towards QCD at Five Loops*, [arXiv:2407.16385].
- [57] M. Laine and A. Vuorinen, *Basics of Thermal Field Theory*, Lect. Notes Phys. **925** (2016), pp.1-281 Springer, 2016, [arXiv:1701.01554].
- [58] A. I. Davydychev and Y. Schröder, *Recursion-free solution for two-loop vacuum integrals with “collinear” masses*, JHEP **12** (2022), 047 [arXiv:2210.10593].
- [59] Y. Schröder, *A fresh look on three-loop sum-integrals*, JHEP **08** (2012), 095 [arXiv:1207.5666].
- [60] J. O. Andersen and L. Kyllingstad, *Four-loop Screened Perturbation Theory*, Phys. Rev. D **78** (2008), 076008 [arXiv:0805.4478].
- [61] I. Ghisoiu and Y. Schröder, *A new three-loop sum-integral of mass dimension two*, JHEP **09**, 016 (2012) [arXiv:1207.6214].
- [62] J. Möller and Y. Schröder, *Open problems in hot QCD*, Nucl. Phys. B Proc. Suppl. **205-206**, 218-223 (2010) [arXiv:1007.1223].
- [63] J. Möller and Y. Schröder, *Three-loop matching coefficients for hot QCD: Reduction and gauge independence*, JHEP **08** (2012), 025 [arXiv:1207.1309].
- [64] I. Ghisoiu, *Three-loop Debye mass and effective coupling in thermal QCD*, PhD. Thesis U. Bielefeld (2013).
- [65] I. Ghisoiu and Y. Schröder, *Automated computation meets hot QCD*, PoS **LL2012** (2012), 063 [arXiv:1210.5415].